The generalized Empirical Interpolation Method: stability theory on Hilbert spaces with an application to the Stokes equation

Yvon Maday, Olga Mula, Anthony T. Patera, Masayuki Yano

The generalized Empirical Interpolation Method: stability theory on Hilbert spaces with an application to the Stokes equation

Maday, Y.[a,b,c,e], Mula, O.[a,d,e,*], Patera, A.T.[f], Yano, M.[f]

[a] *Sorbonne Universités, UPMC Univ Paris 06 and CNRS UMR 7598, Laboratoire Jacques-Louis Lions, F-75005, Paris, France.*
[b] *Institut Universitaire de France*
[c] *Division of Applied Mathematics, Brown University, Providence RI, USA.*
[d] *CEA Saclay, DEN/DANS/DM2S/SERMA/LLPR, 91191 Gif-Sur-Yvette CEDEX - France*
[e] *LRC MANON – CEA/DEN/DANS/DM2S and UPMC-CNRS/LJLL.*
[f] *Department of Mechanical Engineering, Massachusets Institute of Technology, 77 Masachussets Avenue, Cambridge, MA 02139, USA*

Abstract

The Generalized Empirical Interpolation Method (GEIM) is an extension first presented in [1] of the classical empirical interpolation method (see [2], [3], [4]) where the evaluation at interpolating points is replaced by the evaluation at interpolating continuous linear functionals on a class of Banach spaces. As outlined in [1], this allows to relax the continuity constraint in the target functions and expand the application domain. A special effort has been made in this paper to understand the concept of stability condition of the generalized interpolant (the Lebesgue constant) by relating it in the first part of the paper to an inf-sup problem in the case of Hilbert spaces. In the second part, it will be explained how GEIM can be employed to monitor in real time physical experiments by combining the acquisition of measurements from the processes with their mathematical models (parameter-dependent PDE's). This idea will be illustrated through a parameter dependent Stokes problem in which it will be shown that the pressure and velocity fields can efficiently be reconstructed with a relatively low dimension of the interpolating spaces.

Keywords: empirical interpolation; generalized empirical interpolation; reduced basis; model order reduction; stability; Stokes equations

Introduction

Let $\mathcal{X}$ be a Banach space of functions defined over a domain $\overline{\Omega} \in \mathbb{R}^d$ (or $\mathbb{C}^d$), let $(X_n)_n$, $X_n \subset \mathcal{X}$, be a family of finite dimensional spaces, $\dim X_n = n$, and let $(S_n)_n$ be an associated family of sets of points: $S_n = \{x_i^n\}_{i=1}^n$, with $x_i^n \in \overline{\Omega}$. The problem of interpolating any function $f \in \mathcal{X}$ has traditionally been stated as:

$$\text{"Find } f_n \in X_n \text{ such that } f_n(x_i^n) = f(x_i^n),\ \forall i \in \{1, \dots, n\}\text{"}, \tag{1}$$

where we note that it is implicitly required that $\mathcal{X}$ is a Banach space of continuous functions. The most usual approximation in this sense is the Lagrangian interpolation, where the interpolating spaces X_n are of polynomial nature (spanned by plain polynomials, rational functions, Fourier series...) and the question on how to appropriately select the interpolating points in this case has broadly been explored. Although there exists still nowadays open issues on Lagrangian interpolation (see, e.g. [5]), it is also interesting to look for extensions of this procedure in which the interpolating spaces X_n are not necessarily of polynomial nature. The search for new interpolating spaces X_n is therefore linked with the question on how to optimally select the interpolating points in this case and how to obtain a process that is at least stable and close to the best approximation in some sense.

*Corresponding author: O. Mula (Tel: +33 6 11 18 73 89 or +49 24 18 09 65 92)
Email address: mula-hernandez@ann.jussieu.fr (Mula, O.)

Although several procedures have been explored in this direction (we refer to [6], [7] and also to the kriging studies in the stochastic community such as [8]), of particular interest for the present work is the Empirical Interpolation Method (EIM, [2], [3], [4]) that has been developed in the broad framework where the functions f to approximate belong to a compact set F of continuous functions ($\mathcal{X} = C(\Omega)$). The structure of F is supposed to make any $f \in F$ be approximable by finite expansions of small size. This is quantified by the Kolmogorov $n-$width $d_n(F, \mathcal{X})$ of F in $\mathcal{X}$ (see definition 2 below) whose smallness measures the extent to which F can be approximated by some finite dimensional space $X_n \subset \mathcal{X}$ of dimension n. Unfortunately, in general, the best approximation n-dimensional space is not known and, in this context, the Empirical Interpolation Method aims at building a family of suitable enough interpolating spaces X_n together with sets of interpolating points S_n such that the interpolation is well posed. This is done by a greedy algorithm on both the interpolating points and the interpolating selected functions φ_i (see [2]). This procedure has the main advantage of being constructive, i.e. the sequence of interpolating spaces (X_n) and interpolating points (S_n) are hierarchically defined and the procedure can easily be implemented by recursion.

A recent extension of this interpolation process consists in generalizing the evaluation at interpolating points by application of a class of interpolating continuous linear functionals chosen in a given dictionary $\Sigma \subset \mathcal{L}(\mathcal{X})$. This gives rise to the so-called Generalized Empirical Interpolation Method (GEIM). In this new framework, the particular case where the space $\mathcal{X} = L^2(\Omega)$ was first studied in [1]. We also mention the preliminary works of [9] in which the authors introduced the use of linear functionals in EIM in a finite dimensional framework. In the present paper, we will start by revisiting the foundations of the theory in order to show that GEIM holds for Banach spaces $\mathcal{X}$ (section 1). The concept of stability condition (Lebesgue constant, Λ_n) of the generalized interpolant will also be introduced.

In the particular case where $\mathcal{X}$ is a Hilbert space, we will provide an interpretation of the generalized interpolant of a function as an oblique projection. This will shed some light in the understanding of GEIM from an approximation theory perspective (section 2.1). This point of view will be the key to show that the Lebesgue constant is related to an inf-sup problem (section 2.2) that can be easily computed (section 3). The derived formula can be seen as an extension of the classical formula for Lagrangian interpolation to Hilbert spaces. It will also be shown that the Greedy algorithm aims at minimizing the Lebesgue constant in a sense that will be made precise in section 2.3. Furthermore, the inf-sup formula that will be introduced will explicitly show that there exists an interaction between the dictionary Σ of linear functionals and the Lebesgue constant. Although it has so far not been possible to derive a general theory about the impact of Σ on the behavior of the Lebesgue constant, we present in section 4 a first simple example in which this influence is analyzed.

The last part of the paper (section 5) will deal with the potential applications of the method. In particular, we will explain how GEIM can be used to build a tool for the real-time monitoring of a physical or industrial process. This will be done by combining measurements collected from the process itself with a mathematical model (a parameter dependent PDE) that represents our physical understanding of the process under consideration. This idea will be illustrated through a parameter dependent Stokes problem for $\mathcal{X} = \left(H^1(\Omega)\right)^2 \times L^2(\Omega)$.

Taking advantage of this idea, we will outline in the conclusion how the method could be used to build an adaptive tool for the supervision of experiments that could distinguish between normal and accidental conditions. We believe that this tool could help in taking real-time decisions regarding the security of processes.

1. The Generalized Empirical Interpolation Method

Let $\mathcal{X}$ be a Banach space of functions defined over a domain $\Omega \subset \mathbb{R}^d$, where $d = 1, 2, 3$. Its norm is denoted by $\|.\|_{\mathcal{X}}$. Let F be a compact set of $\mathcal{X}$. With $\mathcal{M}$ being some given large number, we assume that the dimension of the vectorial space spanned by F (denoted as $\mathcal{F} = \text{span}\{F\}$) is of dimension larger than $\mathcal{M}$. Our goal is to build a family of n-dimensional subspaces of $\mathcal{X}$ that approximate well enough any element of F. The rationale of this approach is linked to the notion of n-width following Kolmogorov [10]:

Definition 1.1. *Let F be a subset of some Banach space $\mathcal{X}$ and Y_n be a generic n-dimensional subspace of $\mathcal{X}$. The deviation between F and Y_n is*

$$E(F; Y_n) := \sup_{x \in F} \inf_{y \in Y_n} \|x - y\|_{\mathcal{X}} .$$

The Kolmogorov n-width of F in $\mathcal{X}$ is given by

$$\begin{aligned} d_n(F,\mathcal{X}) &:= \inf\{E(F;Y_n) : Y_n \text{ a n-dimensional subspace of } X\} \\ &= \inf_{Y_n} \sup_{x\in F} \inf_{y\in Y_n} \|x-y\|_{\mathcal{X}} . \end{aligned} \tag{2}$$

The smallness of the n-width of F thus measures to what extent the set F can be approximated by an n-dimensional subspace of $\mathcal{X}$. Several reasons can account for a rapid decrease of $d_n(F,\mathcal{X})$: if F is a set of functions defined over a domain, we can refer to regularity, or even to analyticity, of these functions with respect to the domain variable (as analyzed in the example in [10]). Another possibility — that will actually be used in our numerical application— is when $F = \{u(\mu,.),\ \mu \in D\}$, where D is a compact set of $\mathbb{R}^p$ and $u(\mu,.)$ is the solution of a PDE parametrized by μ. The approximation of any element $u(\mu,.) \in F$ by finite expansions is a classical problem addressed by, among others, reduced basis methods and the regularity of u in μ can also be a reason for having a small n-width as the results of [11] and [12] show.

Finally, let us also assume that we have at our disposal a dictionary of linear functionals $\Sigma \subset \mathcal{L}(\mathcal{X})$ with the following properties:

P1: $\forall \sigma \in \Sigma, \|\sigma\|_{\mathcal{L}(\mathcal{X})} = 1$.

P2: *Unisolvence property*: If $\varphi \in \text{span}\{F\}$ is such that $\sigma(\varphi) = 0,\ \forall \sigma \in \Sigma$, then $\varphi = 0$.

Given this setting, GEIM aims at building M-dimensional interpolating spaces X_M spanned by suitably chosen functions $\{\varphi_1, \varphi_2, \ldots, \varphi_M\}$ of F together with sets of M selected linear functionals $\{\sigma_1, \sigma_2, \ldots, \sigma_M\}$ coming from Σ such that any $\varphi \in F$ is well approximated by its generalized interpolant $\mathcal{J}_M[\varphi] \in X_M$ defined by the following interpolation property:

$$\forall \varphi \in \mathcal{X}, \quad \mathcal{J}_M[\varphi] \in X_M \text{ such that } \sigma_i(\mathcal{J}_M[\varphi]) = \sigma_i(\varphi),\ \forall i = 1,\ldots,M. \tag{3}$$

The definition of GEIM in the sense of (3) raises several questions:

- is there an optimal selection for the linear functionals σ_i within the dictionary Σ ?
- is there a constructive optimal selection for the functions $\varphi_i \in F$?
- given a set of linearly independent functions $\{\varphi_i\}_{i\in[1,M]}$ and a set of continuous linear functionals $\{\sigma_i\}_{i\in[1,M]}$, does the interpolant exist in the sense of (3)?
- is the interpolant unique?
- Under what hypothesis can we expect the GEIM approximation to converge rapidly to φ?

In what follows, we provide answers to these questions either with rigorous proofs or with numerical evidences.

The construction of the generalized interpolation spaces X_M and the selection of the suitable associated linear functionals is recursively performed by following a greedy procedure very similar to the one of the classical EIM. The first selected function is, e.g.,

$$\varphi_1 = \arg\sup_{\varphi\in F} \|\varphi\|_{\mathcal{X}},$$

that defines $X_1 = \text{span}\{\varphi_1\}$. The first interpolating linear functional is

$$\sigma_1 = \arg\sup_{\sigma\in\Sigma} |\sigma(\varphi_1)|.$$

The interpolation operator $\mathcal{J}_1 : \mathcal{X} \mapsto X_1$ is defined such that (3) is true for $M = 1$, i.e. $\sigma_1(\mathcal{J}_1[\varphi]) = \sigma_1(\varphi)$, for any $\varphi \in \mathcal{X}$. To facilitate the practical computation of the generalized interpolant, we express it in terms of

$$q_1 = \frac{\varphi_1}{\sigma_1(\varphi_1)},$$

which will be the basis function that will be employed for X_1. In this basis, the interpolant reads

$$\mathcal{J}_1[\varphi] = \sigma_1(\varphi)q_1, \quad \forall \varphi \in \mathcal{X}.$$

We then proceed by induction. With $M_{\max} < \mathcal{M}$ being an upper bound fixed *a priori*, assume that, for a given $1 \leq M < M_{\max}$, we have selected a set of functions $\{\varphi_1, \varphi_2, \ldots, \varphi_M\}$ associated to the basis functions $\{q_1, q_2, \ldots, q_M\}$ and the interpolating linear functionals $\{\sigma_1, \sigma_2, \ldots, \sigma_M\}$. The generalized interpolant is assumed to be well defined by (3), i.e.,

$$\mathcal{J}_M[\varphi] = \sum_{j=1}^{M} \alpha_j^M(\varphi) q_j, \quad \varphi \in \mathcal{X},$$

where the coefficients $\alpha_j^M(\varphi),\ j = 1, \ldots, M$ are given by the interpolation problem

$$\begin{cases} \text{Find } \{\alpha_j^M(\varphi)\}_{j=1}^M \text{ such that:} \\ \sum\limits_{j=1}^{M} \alpha_j^M(\varphi) B_{i,j}^M = \sigma_i(\varphi),\ \forall i = 1, \ldots, M. \end{cases}$$

where $B_{i,j}^M$ are the coefficients of the $M \times M$ matrix $B^M := \left(\sigma_i(q_j)\right)_{1 \leq i,j \leq M}$. We now define

$$\forall \varphi \in F, \quad \varepsilon_M(\varphi) = \|\varphi - \mathcal{J}_M[\varphi]\|_{\mathcal{X}}.$$

At the $M+1$-th stage of the greedy algorithm, we choose φ_{M+1} such that

$$\varphi_{M+1} = \arg\sup_{\varphi \in F} \varepsilon_M(\varphi) \tag{4}$$

and

$$\sigma_{M+1} = \arg\sup_{\sigma \in \Sigma} |\sigma(\varphi_{M+1} - \mathcal{J}_M[\varphi_{M+1}])|. \tag{5}$$

The next basis function is then:

$$q_{M+1} = \frac{\varphi_{M+1} - \mathcal{J}_M[\varphi_{M+1}]}{\sigma_{M+1}(\varphi_{M+1} - \mathcal{J}_M[\varphi_{M+1}])}.$$

We finally set $X_{M+1} \equiv \text{span}\{\varphi_j,\ 1 \leq j \leq M+1\} = \text{span}\{q_j,\ 1 \leq j \leq M+1\}$. The interpolation operator $\mathcal{J}_{M+1} : \mathcal{X} \mapsto X_{M+1}$ is given by

$$\mathcal{J}_{M+1}[\varphi] = \sum_{j=1}^{M+1} \alpha_j^{M+1}(\varphi) q_j, \quad \forall \varphi \in \mathcal{X},$$

so as to satisfy (3). The coefficients $\alpha_j^{M+1}(\varphi),\ j = 1, \ldots, M+1$, are therefore given by the interpolation problem

$$\begin{cases} \text{Find } \{\alpha_j^{M+1}(\varphi)\}_{j=1}^{M+1} \text{ such that:} \\ \sum\limits_{j=1}^{M+1} \alpha_j^{M+1}(\varphi) B_{i,j}^{M+1} = \sigma_i(\varphi),\ \forall i = 1, \ldots, M+1, \end{cases}$$

where $B^{M+1} = \left(\sigma_i(q_j)\right)_{1 \leq i,j \leq M+1}$.

By following exactly the same guidelines as in [1] where the particular case $\mathcal{X} = L^2(\Omega)$ was addressed, it can be proven that, in the general case where $\mathcal{X}$ is a Banach space, the generalized interpolation is well-posed: for any $1 \leq M < \mathcal{M}$, the set of functions $\{q_j,\ j \in [1, M]\}$ is linearly independent and therefore the space X_M is of dimension M. Furthermore, the matrix B^M is lower triangular with unity diagonal (hence invertible) with off-diagonal entries in $[-1, 1]$.

Note that GEIM reduces to EIM if $\mathcal{X} = C^0(\Omega)$ and Σ is composed of Dirac masses. Also, if the cardinality $\#F$ of F is finite, then the Greedy algorithm is exact in the sense that $F \subset X_{\#F}$. This type of property does not hold in traditional Lagrangian interpolation due to the fact that the interpolating polynomial spaces are used to interpolate continuous

functions that are not necessarily of polynomial nature. Finally, note also that the approach can be shortcut if the basis functions are available, in which case the interpolating linear functionals/points are the only output of GEIM/EIM.

It is also important to point out that the current extension of EIM presents two major advantages: first, it allows the interpolation of functions of weaker regularity than $\mathcal{C}^0(\Omega)$. The second interest is related to the potential applications of GEIM: the use of linear functionals can model in a more faithful manner real sensors involved in physical experiments (indeed, these are in practice no point evaluations as it is usually supposed but rather local averages of some quantity of interest). The potentialities of these two aspects will be illustrated in the numerical application presented in section 5.

We now state a first result about the interpolation error of GEIM.

Theorem 1.2 (Interpolation error on a Banach space)**.** *$\forall \varphi \in \mathcal{X}$, the interpolation error satisfies:*

$$\|\varphi - \mathcal{J}_M[\varphi]\|_{\mathcal{X}} \leq (1 + \Lambda_M) \inf_{\psi_M \in X_M} \|\varphi - \psi_M\|_{\mathcal{X}}, \tag{6}$$

where

$$\Lambda_M := \|\mathcal{J}_M\|_{\mathcal{L}(\mathcal{X})} = \sup_{\varphi \in \mathcal{X}} \frac{\|\mathcal{J}_M[\varphi]\|_{\mathcal{X}}}{\|\varphi\|_{\mathcal{X}}} \tag{7}$$

is the Lebesgue constant in the $\mathcal{X}$ norm.

Proof. The desired result easily follows since for any $\varphi \in \mathcal{X}$ and any $\psi_M \in X_M$ we have:

$$\begin{aligned} \|\varphi - \mathcal{J}_M[\varphi]\|_{\mathcal{X}} &= \|[\varphi - \psi_M] - \mathcal{J}_M[\varphi - \psi_M]\|_{\mathcal{X}} \\ &\leq \|I_F - \mathcal{J}_M\|_{\mathcal{L}(\mathcal{X})} \|\varphi - \psi_M\|_{\mathcal{X}} \\ &\leq (1 + \|\mathcal{J}_M\|_{\mathcal{L}(\mathcal{X})}) \|\varphi - \psi_M\|_{\mathcal{X}}, \end{aligned}$$

which yields the desired inequality. □

The last term in the right hand side of equation (6) is known as the best fit of φ by elements in the space X_M. However, X_M does not in general coincide with the optimal M-dimensional space in the sense that $X_M \neq X_M^{\text{opt}}$, with $X_M^{\text{opt}} = \underset{\substack{Y_M \subset \mathcal{X} \\ \dim(Y_M)=M}}{\arg\inf} E(F, Y_M)$. This raises the question of the quality of the finite dimensional subspaces X_M provided by the Greedy selection procedure. It has been proven first in [13] in the case of $\mathcal{X} = L^2(\Omega)$ and then in [14] in a general Banach space that the interpolating spaces X_M coming from the Greedy selection procedure of GEIM are quite optimal and that the lack of optimality comes from the Lebesgue constant. The main results are the following (see [14]):

Theorem 1.3 (See corollary 3.13 of [14])**.**

i) If $d_M(F, \mathcal{X}) \leq C_0 M^{-\alpha}$, $M = 1, 2, \ldots$ and that $(1 + \Lambda_M) \leq C_\zeta M^\zeta$, for any $M = 1, 2, \ldots$, then the interpolation error satisfies for any $\varphi \in F$ the inequality $\|\varphi - \mathcal{J}_M[\varphi]\|_{\mathcal{X}} \leq C_\zeta C_1 M^{-\alpha+2\zeta+\beta}$, where

$$C_1 := \max\left\{ C_0 2^{\frac{2\alpha^2}{\zeta}} \left(\frac{\zeta+\beta}{\beta-\frac{1}{2}}\right)^\alpha \max\left(1; C_\zeta^{\frac{\zeta+\beta}{\zeta}}\right); \max_{M=1,\ldots,2\lfloor 2(\zeta+\beta)\rfloor+1} M^{\alpha-\zeta-\beta} \right\}.$$

ii) If (Λ_M) is a monotonically increasing sequence and if $d_M(F, \mathcal{X}) \leq C_0 e^{-c_1 M^\alpha}$ for any $M \geq 1$, then, for any $\varphi \in F$, the interpolation error can be bounded as

$$\|\varphi - \mathcal{J}_M[\varphi]\|_{\mathcal{X}} \leq \begin{cases} 4C_0(1 + \Lambda_1), & \text{if } M = 1. \\ \sqrt{2C_0}(1 + \Lambda_M)^2 \sqrt{M} e^{-c_2 M^\alpha}, & \text{if } M \geq 2. \end{cases}$$

As a consequence of this result, the interpolation error of GEIM will converge if the Lebesgue constant "does not increase too fast" in the sense that it allows that the previous upper bounds tend to zero as the dimension M increases. By following the same lines as in [1], it can be proven that when $\mathcal{X}$ is a Banach space, the Lebesgue constant has the exponential upper-bound

$$\Lambda_M \leq 2^{M-1} \max_{i\in[1,M]} \|q_i\|_{\mathcal{X}}, \tag{8}$$

which implies that the decay of $d_M(F,\mathcal{X})$ should be exponential in order to converge. However, the behavior of $(\Lambda_M)_M$ observed in numerical applications (see section 5) is rather linear and leads us to expect that the upper bound of (8) is far from being optimal in a class of set F of small Kolmogorov n-width.

2. Further results in the case of a Hilbert space

In this section $\mathcal{X}$ is a Hilbert space of functions where the norm $\|.\|_{\mathcal{X}}$ is induced by the inner product $(\cdot,\cdot)_{\mathcal{X}}$. We will see that in this case the generalized interpolant can been seen as an oblique projection. It will also be proven that we can derive a sharp interpolation error bound in this case. An explicit (and easily computable) formula for the Lebesgue constant will also be obtained and this formula will be used to show that the Greedy algorithm aims at minimizing the Lebesgue constant.

2.1. Interpretation of GEIM as an oblique projection

For $1 \leq j \leq M$, if σ_j is the j^{th}-linear functional selected by the greedy algorithm, let w_j be its Riesz representation in $\mathcal{X}$, i.e. w_j is such that

$$\forall \varphi \in \mathcal{X}, \quad \sigma_j(\varphi) = (w_j, \varphi)_{\mathcal{X}}. \tag{9}$$

It follows from the well posedness of the generalized interpolation that $\{\sigma_1,\dots,\sigma_M\}$ are linearly independent and therefore $\{w_1,\dots,w_M\}$ are also linearly independent. With these notations, we can provide the following interpretation of the generalized interpolant of a function (see figure 1 for a schematic representation):

Lemma 2.1. *$\forall f \in \mathcal{X}$, $\mathcal{J}_M[f]$ is an oblique projection onto the space X_M orthogonal to the M-dimensional space $W_M = \text{span}\{w_1,\dots,w_M\}$, i.e.*

$$(\mathcal{J}_M(f) - f, w)_{\mathcal{X}} = 0, \ \forall w \in W_M. \tag{10}$$

Proof. For any $f \in \mathcal{X}$, the interpolation property reads $\sigma_j(f) = \sigma_j(\mathcal{J}_M[f])$, for $1 \leq j \leq M$. It is then clear that $(w_j, f)_{\mathcal{X}} = (w_j, \mathcal{J}_M[f])_{\mathcal{X}}$ and the result easily follows from the fact that $\{w_1,\dots,w_M\}$ are a basis of W_M. □

A direct consequence of lemma 2.1 is the following result:

Corollary 2.2. *If $\Sigma = (\text{span}\{F\}^{\perp})^{\circ}$, then $W_M = X_M$ and the resulting generalized interpolant is the orthogonal projection of f onto the space X_M.*

Proof. If $\Sigma = (\text{span}\{F\}^{\perp})^{\circ}$, then, from the arg max definition of σ_k in the greedy algorithm, the Riesz representation of σ_k is the function $w_k = \varphi_k - \mathcal{J}_{k-1}(\varphi_k)$ for $k \geq 2$ and $w_1 = \varphi_1$ if $k = 1$. The interpolation property $\sigma_k(f - \mathcal{J}_M(f)) = 0$ implies in this case that $(w_k, f - \mathcal{J}_{k-1}(f))_{\mathcal{X}}$ for any $k \in \{1,\dots,M\}$. But since the family $\{w_1,\dots,w_M\}$ is a basis of X_M in this particular case, it follows that $(f - \mathcal{J}_M(f), w)_{\mathcal{X}} = 0$ for all $w \in X_M$. □

Remark 2.3. *The case $\Sigma = (\text{span}\{F\}^{\perp})^{\circ}$ is a theoretical situation that does not usually hold in practical applications. Corollary 2.2 is however a first step towards the theoretical understanding of the impact of the dictionary Σ on the interpolation procedure.*

From lemma 2.1, note that $\mathcal{J}_M[f]$ can also be seen as a particular Petrov-Galerkin approximation of the function f in the case where the approximation space is X_M and the trial space is W_M. Indeed, the search for the generalized interpolant can be stated as:

$$\begin{cases} \text{Given } f \in \mathcal{X}, \text{ find } \mathcal{J}_M[f] \in X_M \text{ such that} \\ (\mathcal{J}_M[f], w)_{\mathcal{X}} = (f, w)_{\mathcal{X}}, \quad \forall w \in W_M. \end{cases} \tag{11}$$

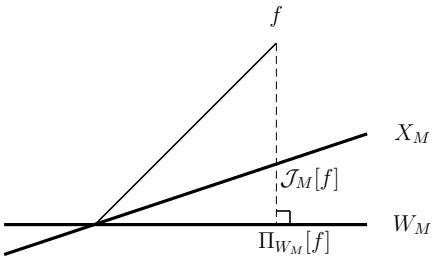

Figure 1: Interpretation of $\mathcal{J}_M[f]$ as an oblique projection.

This formulation leads to the classical error estimation:

$$\|f - \mathcal{J}_M[f]\|_{\mathcal{X}} \leq \left(1 + \frac{1}{\beta_M}\right) \inf_{\psi_M \in X_M} \|f - \psi_M\|_{\mathcal{X}}, \tag{12}$$

where β_M is the inf-sup constant

$$\beta_M := \inf_{x \in X_M} \sup_{w \in W_M} \frac{(x, w)_{\mathcal{X}}}{\|x\|_{\mathcal{X}} \|w\|_{\mathcal{X}}}. \tag{13}$$

It will be proven in the next section that the parameter $1/\beta_M$, which is, in fact, equal to the Lebesgue constant Λ_M. We will also see that the error bound provided in relation (12) is slightly suboptimal due to the presence of the coefficient 1 before the parameter $1/\beta_M$.

2.2. Interpolation error

The interpretation of the generalized interpolant as an oblique projection is useful to derive the following result about the interpolation error:

Theorem 2.4 (Interpolation error on a Hilbert space)**.** *$\forall \varphi \in \mathcal{X}$, the interpolation error satisfies the sharp upper bound:*

$$\|\varphi - \mathcal{J}_M[\varphi]\|_{\mathcal{X}} \leq \Lambda_M \inf_{\psi_M \in X_M} \|\varphi - \psi_M\|_{\mathcal{X}} \tag{14}$$

where $\Lambda_M := \|\mathcal{J}_M\|_{\mathcal{L}(\mathcal{X})} = \sup_{\varphi \in \mathcal{X}} \dfrac{\|\mathcal{J}_M[\varphi]\|_{\mathcal{X}}}{\|\varphi\|_{\mathcal{X}}}$ is the Lebesgue constant in the $\mathcal{X}$ norm. Furthermore, $\Lambda_M = \dfrac{1}{\beta_M}$, where

$$\beta_M := \inf_{x \in X_M} \sup_{w \in W_M} \frac{(x, w)_{\mathcal{X}}}{\|x\|_{\mathcal{X}} \|w\|_{\mathcal{X}}}. \tag{15}$$

Proof. Let $\nu_M := \inf_{w^\perp \in W_M^\perp} \sup_{x^\perp \in X_M^\perp} \dfrac{(w^\perp, x^\perp)_{\mathcal{X}}}{\|w^\perp\|_{\mathcal{X}} \|x^\perp\|_{\mathcal{X}}}$. It is immediate that

$$\forall w^\perp \in W_M^\perp, \quad \nu_M \|w^\perp\|_{\mathcal{X}} \leq \sup_{x^\perp \in X_M^\perp} \frac{(w^\perp, x^\perp)_{\mathcal{X}}}{\|x^\perp\|_{\mathcal{X}}}.$$

Furthermore, for any $\varphi \in \mathcal{X}$, it follows from lemma 2.1 that $\varphi - \mathcal{J}_M[\varphi] \in W_M^\perp$. Then:

$$\nu_M \|\varphi - \mathcal{J}_M[\varphi]\|_{\mathcal{X}} \leq \sup_{x^\perp \in X_M^\perp} \frac{(\varphi - \mathcal{J}_M[\varphi], x^\perp)_{\mathcal{X}}}{\|x^\perp\|_{\mathcal{X}}}. \tag{16}$$

Besides, for any $x \in X_M$ and any $x^\perp \in X_M^\perp$:

$$(\varphi - x, x^\perp)_{\mathcal{X}} = (\varphi - \mathcal{J}_M[\varphi], x^\perp)_{\mathcal{X}}\,. \tag{17}$$

The Cauchy-Schwarz inequality applied to (16) combined with relation (17) yields:

$$\nu_M \|\varphi - \mathcal{J}_M[\varphi]\|_{\mathcal{X}} \leq \inf_{x \in X_M} \|\varphi - x\|_{\mathcal{X}}. \tag{18}$$

Next, it can be proven (see corollary Appendix A.1 in appendix) that $\nu_M = \beta_M$, which yields the inequality

$$\|\varphi - \mathcal{J}_M[\varphi]\|_{\mathcal{X}} \leq \frac{1}{\beta_M} \inf_{\psi_M \in X_M} \|\varphi - \psi_M\|_{\mathcal{X}}. \tag{19}$$

The end of the proof consists in showing that $\frac{1}{\beta_M} = \Lambda_M = \sup_{\varphi \in \mathcal{X}} \frac{\|\mathcal{J}_M[\varphi]\|_{\mathcal{X}}}{\|\varphi\|_{\mathcal{X}}}$. This is done by noting first of all that formula (15) implies that

$$\forall \varphi \in \mathcal{X}, \quad \beta_M \|\mathcal{J}_M[\varphi]\|_{\mathcal{X}} \leq \sup_{w \in W_M} \frac{(\mathcal{J}_M[\varphi], w)_{\mathcal{X}}}{x} \leq \|\mathcal{J}_M[\varphi]\|_{\mathcal{X}},$$

where we have used the fact that $(\mathcal{J}_M[\varphi], w)_{\mathcal{X}} = (\varphi, w)_{\mathcal{X}}$ for all $w \in W_M$ and the Cauchy-Schwarz inequality. Therefore,

$$\forall \varphi \in \mathcal{X}, \ \|\mathcal{J}_M[\varphi]\|_{\mathcal{X}} \leq \frac{1}{\beta_M} \|\varphi\|_{\mathcal{X}},$$

which implies that $\Lambda_M \leq \frac{1}{\beta_M}$.

Let us now denote by v_M an element of X_M with norm $\|v_M\|_{\mathcal{X}} = 1$ such that

$$\sup_{w_M \in W_M} \frac{(v_M, w_M)_{\mathcal{X}}}{\|w_M\|_{\mathcal{X}}} = \beta_M.$$

If we call w_M^* the $\mathcal{X}$ projection of v_M over W_M, then

$$v_M = w_M^* + \tilde{w}_M^*,$$

with $w_M^* \in W_M$ and $\tilde{w}_M^* \in W_M^{\perp}$, so that $(w_M^*, \tilde{w}_M^*) = 0$. We have $\mathcal{J}_M(w_M^*) = v_M$. Indeed, by definition $\mathcal{J}_M[w_M^*] \in X_M$ and $\forall w_M \in W_M$, $(\mathcal{J}_M[w_M^*], w_M)_{\mathcal{X}} = (w_M^*, w_M)_{\mathcal{X}}$, which is exactly what v_M satisfies. In addition, $\sup_{w_M \in W_M} \frac{(v_M, w_M)_{\mathcal{X}}}{\|w_M\|_{\mathcal{X}}}$ is achieved for $w_M = w_M^*$ so that $\|w_M^*\|_{\mathcal{X}} = \beta_M$. This ends the proof that

$$1 = \|v_M\|_{\mathcal{X}} = \|\mathcal{J}_M[w_M^*]\|_{\mathcal{X}} = \frac{1}{\beta_M} \|w_M^*\|_{\mathcal{X}}.$$

Since the above result implies that $\frac{1}{\beta_M} \leq \Lambda_M$, we conclude that $\frac{1}{\beta_M} = \Lambda_M$.

□

Remark 2.5. *The link between the Lebesgue constant Λ_M and the inf-sup quantity β_M introduced in theorem 2.4 shows that Λ_M depends on the dictionary of linear functionals Σ and also on the interpolating space X_M. Although no theoretical analysis of the impact of these elements has been possible so far, we present in section 4 a numerical study about the influence of the dictionary Σ in Λ_M.*

Remark 2.6. *Note that, since theorem 2.4 holds only in Hilbert spaces, formula (15) does not apply to the Lebesgue constant of the classical EIM given that it is defined in the $L^\infty(\Omega)$ norm. The Hilbertian framework allows nevertheless to consider Dirac masses as linear functionals like in EIM if we place ourselves, e.g., in $H^2(\Omega)$.*

2.3. The Greedy algorithm aims at optimizing the Lebesgue constant

If we look in detail at the steps followed by the Greedy algorithm, once X_{M-1} and W_{M-1} have been derived, the construction of X_M and W_M starts by adding an element φ to X_{M-1}. In the Greedy process, this is done following formula (4), but let us analyze what happens when we add any $\varphi_M \in F$. The first consequence of its addition is that the resulting inf-sup constant becomes zero:

$$\inf_{\varphi \in \text{span}\{X_{M-1}, \varphi_M\}} \sup_{w \in W_{M-1}} \frac{(\varphi, w)_{\mathcal{X}}}{\|\varphi\|_{\mathcal{X}} \|w\|_{\mathcal{X}}} = 0. \tag{20}$$

Indeed, the addition of φ_M to the interpolating basis functions has the consequence of adding the element $\tilde{\varphi}_M = \varphi_M - \mathcal{J}_{M-1}[\varphi_M]$ that, by definition, is such that $(\tilde{\varphi}_M, w)_{\mathcal{X}} = 0,\ \forall w \in W_{M-1}$. We thus need to add an element to W_{M-1} in order to stabilize the inf-sup condition.

Let us denote by W the set of Riesz representations in $\mathcal{X}$ of the elements of our dictionary Σ. Since

$$\inf_{\varphi \in X_{M-1} + \varphi_M} \sup_{w \in W_{M-1}} \frac{(\varphi, w)_{\mathcal{X}}}{\|\varphi\|_{\mathcal{X}} \|w\|_{\mathcal{X}}}$$

is reached by $\tilde{\varphi}_M$, the aim is to add an element w_M of W that maximizes

$$\max_{w \in W} \frac{(\tilde{\varphi}_M, w)_{\mathcal{X}}}{\|w\|_{\mathcal{X}}}. \tag{21}$$

Since the elements of the dictionary are of norm 1 (see property P1 above), this corresponds exactly to one of the steps performed by the Greedy algorithm (see equation (5)). Furthermore, from the unisolvence property of our dictionary, the application

$$\begin{aligned} \|.\|_* : \mathcal{X} &\mapsto \mathbb{R} \\ \varphi &\mapsto \max_{w \in W} (\varphi, w)_{\mathcal{X}} \end{aligned}$$

defines a norm in $\mathcal{X}$. Then, formula (21) reads:

$$\max_{w \in W} \frac{(\tilde{\varphi}_M, w)_{\mathcal{X}}}{\|w\|_{\mathcal{X}}} = \|\varphi_M - \mathcal{J}_{M-1}[\varphi_M]\|_*.$$

It is thus clear that the choice of φ_M that maximizes the value of β_M is the one that maximizes $\varphi_M - \mathcal{J}_{M-1}[\varphi_M]$ in the $\|.\|_*$ norm. However, since in practice we do not have access to the entire knowledge of this norm, $\|.\|_*$ is replaced by the ambient norm $\|.\|_{\mathcal{X}}$:

$$\varphi_M = \arg\max_{\varphi \in F} \|\varphi - \mathcal{J}_{M-1}[\varphi]\|_* \sim \arg\max_{\varphi \in F} \|\varphi - \mathcal{J}_{M-1}[\varphi]\|_{\mathcal{X}}, \tag{22}$$

which is exactly what the Greedy algorithm does (see (4)). Hence, as a conclusion, with the practical tools that can be implemented, the choice of φ_M aims at minimizing the Lebesgue constant with the approximation explained in (22).

3. Practical implementation of the Greedy algorithm and the Lebesgue constant

In the present section, we discuss about some practical issues regarding the implementation of the Greedy algorithm and the Lebesgue constant Λ_M.

Since the cardinality of F is usually infinite, the practical implementation of the Greedy algorithm is carried out in a large enough sample subset $\mathcal{S}_F$ of finite cardinality $\#\mathcal{S}_F$ much larger than the dimension of the discrete spaces X_M and W_M we plan to use. For example, if $F = \{u(\mu, .), \mu \in \mathcal{D}\}$, we choose $\mathcal{S}_F = \{u(\mu, .), \mu \in \Xi_\mu \subset \mathcal{D}\}$ and Ξ_μ consists of $\#\mathcal{S}_F$ parameter sample points μ. We assume that this sample subset is representative enough of the entire set F in the sense that $\sup_{x \in F} \left\{ \inf_{y \in \text{span}\{\mathcal{S}_F\}} \|x - y\|_{\mathcal{X}} \right\}$ is much smaller than the accuracy we envision through the interpolation process. This assumption is valid for small dimension of F, or, more precisely, for small dimension of the parameter set $\mathcal{D}$. In

case it cannot be implemented directly, we can follow two strategies that have been introduced on greedy approaches for reduced basis approximations either based on (parameter) domain decomposition like in [15] or [16] based on an adaptive construction of the sample subset, starting from a very coarse definition as in [17]. These approaches have not been implemented here but we do not foresee any difficulty in adopting them to the GEIM framework.

The following lemma shows that the generalized interpolant can be recursively computed.

Lemma 3.1. *For any function $f \in \mathcal{X}$, we have the following recursion for $M \geq 1$*

$$\begin{cases} \mathcal{J}_M[f] = \mathcal{J}_{M-1}[f] + \sigma_M(f - \mathcal{J}_{M-1}[f])q_M \\ \mathcal{J}_0[f] = 0 \end{cases} \tag{23}$$

and the generalized interpolant of f can be recursively computed.

Proof. Using the fact that the spaces X_M are hierarchically defined, both hand sides of (23) belong to X_M. Using the fact that $\sigma_i(q_M) = 0$ for $i < M$ and the definition of $\mathcal{J}_M$ and $\mathcal{J}_{M-1}$, we infer that

$$\sigma_i\left(\mathcal{J}_M[f]\right) = \sigma_i\left(\mathcal{J}_{M-1}[f] + \sigma_M\left(f - \mathcal{J}_{M-1}[f]\right) q_M\right), \quad \forall i < M.$$

Finally, it is clear that the right and left and sides have the same image trough σ_M. The equality holds by uniqueness of the generalized interpolation procedure.

□

Remark 3.2. *This result also holds for the classical EIM case.*

The greedy algorithm is in practice a very time-consuming task whose computing time could significantly be reduced by the use of parallel architectures and the use of formula (23) as is outlined in algorithm 1.

Once X_M and W_M have been constructed thanks to algorithm 1, the Lebesgue constant can be computed by the resolution of an eigenvalue problem as is explained in

Lemma 3.3. *If $\{\tilde{q}_1, \ldots, \tilde{q}_M\}$ and $\{\tilde{w}_1, \ldots, \tilde{w}_M\}$ are orthonormal basis of X_M and W_M respectively, then*

$$\beta_M = 1/\Lambda_M = \sqrt{\lambda_{\min}(A^T A)}, \tag{24}$$

where A is the $M \times M$ matrix whose entries are $A_{i,j} = (\tilde{w}_i, \tilde{q}_j)_{\mathcal{X}}$ and $\lambda_{\min}(A^T A)$ denotes the minimum eigenvalue of the positive definite matrix $A^T A$.

Proof. Since

$$\beta_M = \inf_{x \in X_M} \sup_{w \in W_M} \frac{(x, w)_{\mathcal{X}}}{\|x\|_{\mathcal{X}} \|w\|_{\mathcal{X}}} = \inf_{x \in \mathbb{R}^M} \sup_{w \in \mathbb{R}^M} \frac{(Ax, w)_2}{\|x\|_2 \|w\|_2} = \inf_{x \in \mathbb{R}^M} \frac{\|Ax\|_2}{\|x\|_2},$$

the result easily follows because $\dfrac{\|Ax\|_2^2}{\|x\|_2^2}$ is the Rayleigh quotient of $A^T A$ whose infimum is achieved by $\lambda_{\min}(A^T A)$. □

Remark 3.4. *Note that β_M corresponds to the minimum singular value of the matrix A, which is a matrix of small size $M \times M$. Its computation can be easily performed by, e.g., the inverse power method.*

4. A numerical study about the impact of the dictionary Σ of linear functionals in the Lebesgue constant

As outlined in remark 2.5, the explicit expression of the Lebesgue constant presented in formula (15) shows that Λ_M is intimately linked to the dictionary of linear functionals Σ that is used in the Greedy algorithm to build the interpolation process. With the exception of the trivial case considered in corollary 2.2, no theoretical analysis of the impact of Σ in the behavior of the Lebesgue constant has been possible so far. For this reason, we present here some numerical results on this issue as a first illustration of this connection. The same computations will also let us numerically validate the formula (15) for Λ_M, whose original definition is given by (7).

Algorithm 1 Practical implementation of the Greedy procedure

Input: $\Sigma,\ \mathcal{S}_F = \{f_k \in F\}_{k=1}^{\#S_F},\ \varepsilon_{tol},\ M_{\max}, M = 0$
Assign a set of functions $\{f_{k_{p,start}}, \dots, f_{k_{p,stop}}\}$ to each processor p.
repeat
  $M \leftarrow M + 1$
  $\varepsilon_{p,\max} = 0$ ▷ *parallel*
  for $k = \{k_{p,start}, \dots, k_{p,stop}\}$ **do**
    $f = f_k$
    Compute and store $\sigma_M(f - \mathcal{J}_M(f))$.
    Assemble $\mathcal{J}_{M+1}(f)$ following formula (23)
    Compute $\varepsilon_{M+1} = \|f - \mathcal{J}_{M+1}(f)\|_X$
    if $\varepsilon_{M+1} > \varepsilon_{p,\max}$ **then**
      $k_{p,\max} = k$ and $\varepsilon_{p,\max} = \varepsilon_{M+1}$
    end if
  end for ▷ *end parallel*
  Gather $\left\{(\varepsilon_{p,\max}, k_{p,\max})\right\}_{p=1}^{N_{proc}}$ and find $(\varepsilon_{\max}, k_{\max}) = \underset{p\in\{1,\dots,N_{proc}\}}{\arg\max}\ (\varepsilon_{p,\max}, k_{p,\max})$.
  $r_{M+1} = f_{k_{\max}} - \mathcal{J}_M(f_{k_{\max}})$
  $\tilde{\varepsilon}_{p,\max} = 0$ ▷ *parallel*
  for $j = \{j_{p,start}, \dots, j_{p,stop}\}$ **do**
    $\sigma = \sigma_j$
    Compute $\tilde{\varepsilon}_{M+1} = |\sigma(r_{M+1})|$
    if $\tilde{\varepsilon}_{M+1} > \tilde{\varepsilon}_{p,\max}$ **then**
      $j_{p,\max} = j$ and $\tilde{\varepsilon}_{p,\max} = \tilde{\varepsilon}_{M+1}$
    end if
  end for ▷ *end parallel*
  Gather $\left\{(\tilde{\varepsilon}_{p,\max}, j_{p,\max})\right\}_{p=1}^{N_{proc}}$ and find $(\tilde{\varepsilon}_{\max}, j_{\max}) = \underset{p\in\{1,\dots,N_{proc}\}}{\arg\max}\ (\tilde{\varepsilon}_{p,\max}, j_{p,\max})$.
  Compute and store $q_{M+1} = \dfrac{r_{M+1}}{\sigma_{j_{\max}}(r_{M+1})}$.
  Store $\sigma_{M+1} = \sigma_{j_{\max}}$.
  Compute and store w_{M+1} (Riesz representation of σ_{M+1}).
until $\varepsilon_{\max} < \varepsilon_{tol}$ or $M > M_{\max}$
Output: $\{\sigma_1, \dots, \sigma_{M+1}\},\ W_{M+1} = \text{span}\{w_1, \dots, w_{M+1}\},\ X_{M+1} = \text{span}\{q_1, \dots, q_{M+1}\}$.

We place ourselves in $\Omega = [0, 1]$ and consider the numerical approximation in $L^2(\Omega)$ or $H^1(\Omega)$ of the following compact set:

$$F = \{f(., \mu_1, \mu_2) \mid (\mu_1, \mu_2) \in [0.01, 24.9] \times [0, 15]\}, \tag{25}$$

where

$$f(x, \mu_1, \mu_2) = \frac{1}{\sqrt{1 + (25 + \mu_1 \cos(\mu_2 x))x^2}}, \quad \forall x \in \Omega.$$

We remind that $L^2(\Omega) = \{f \mid \|f\|_{L^2(\Omega)} < \infty\}$, where the norm $\|\cdot\|_{L^2(\Omega)}$ is induced by the inner product $(w, v)_{L^2(\Omega)} = \int_\Omega w(x)v(x)dx$. Also, $H^1(\Omega) = \{f \mid \|f\|_{H^1(\Omega)} < \infty\}$, where the norm $\|\cdot\|_{H^1(\Omega)}$ is induced by the inner product $(w, v)_{H^1(\Omega)} = \int_\Omega w(x)v(x)dx + \int_\Omega \nabla w(x).\nabla v(x)dx$.

Any $f \in F$ will be approximated by its generalized interpolant at dimension M. For this purpose, the practical construction of the interpolating space X_M and the selection of the linear functionals is done through the Greedy algorithm described in section 3. The following dictionary of linear functionals has been employed:

$$\Sigma = \{\sigma_k \in \mathcal{L}(X),\ k \in \{1, \dots, N_{sensor}\}\}, \tag{26}$$

where $N_{sensor} = 150$, and

$$\sigma_k(\varphi) = \int_{x\in\Omega} c_{k,s}(x)\varphi(x)dx, \quad \forall \varphi \in \mathcal{X}. \tag{27}$$

The function $c_{k,s}$ reads:

$$c_{k,s}(x) = \frac{m_{k,s}(x)}{\|m_{k,s}(x)\|_{L^1(\Omega)}}, \quad \forall x \in \Omega,$$

where

$$m_{k,s}(x) := e^{-(x-x_k)^2/(2s^2)}, \quad \forall x \in \Omega$$

and $x_k \in \Omega$. We will explore the variation of the coefficient $s \in \mathbb{R}_+$ in order to understand the influence of the dictionary Σ on Λ_M.

4.1. Validation of the inf-sup formula

We will first start by fixing s to a value of 0.005 and by numerically validating formula (15) of the Lebesgue constant by comparing it to the value given by the original formula (7).

Regarding the computation of (15), the quantity β_M has been derived using formula (24) of lemma 3.3. It suffices to evaluate the scalar products of the matrix A defined in that lemma and obtain the minimum eigenvalue of A^TA. For the practical computations, a $\mathbb{P}_1$ finite element approximation of the functions $\tilde{q}_i$ and $\tilde{w}_i$ has been used in order to simplify the scalar product evaluation in the L^2 and H^1 spaces. For the same reason and as a matter of global coherence, the computation of the original formula of the Lebesgue constant $\sup_{\varphi\in\mathcal{X}} \frac{\|\mathcal{I}_M[\varphi]\|_{\mathcal{X}}}{\|\varphi\|_{\mathcal{X}}}$ has also involved the same $\mathbb{P}_1$ finite element approximation of the elements of $\mathcal{X}$. This approach leads to the computation of a discrete Raleigh quotient, whose derivation is explained in detail in appendix B.

The results of the computation are given in figure 2 and show an excellent agreement between both values in L^2 and H^1. The same agreement holds for any value of the parameter s of the linear functionals, but, as will be presented in the next section, the behavior of Λ_M varies depending on this parameter.

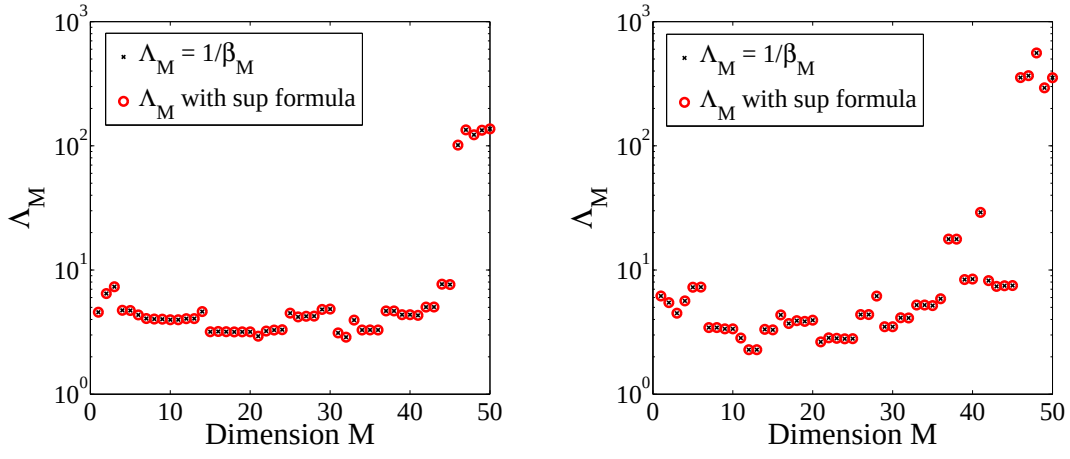

(a) $\mathcal{X} = L^2([0;1])$ **(b)** $\mathcal{X} = H^1([0;1])$

Figure 2: Numerical validation of the inf-sup formula: comparison between formulae (7) and (15).

In the particular case presented here, the behavior of the Lebesgue constant does not significantly change if we place us in L^2 or in H^1 and Λ_M remains constant (the degradation in the behavior for $M \geq 44$ is due to numerical round-off errors).

4.2. Impact of the dictionary of linear functionals

We now study the impact of s on the evolution of the Lebesgue constant through our example in one dimension. For this purpose, we present in figures 3a and 3b the behavior in L^2 and in H^1 of Λ_M for different values of s.

To begin with, we will focus on the behavior for sufficiently large values of s and analyze the range $s \geq 5.10^{-3}$. It can be observed that, as s increases, the behavior of the Lebesgue constant is progressively degraded in both norms. The sequence (Λ_M) starts to diverge at dimensions that are lower and lower as s increases (compare, e.g., the behaviors between the case $s = 2.10^{-2}$ and $s = 4.10^{-2}$). An intuitive manner to interpret this observation is as follows: the dictionary under consideration in this example (see formula (26)) consists on local averages operations whose "range" is controlled by s. As s increases, the range increases and a limit will be reached in which the addition of more linear functionals will result in a redundant addition of information because of an overlap of the domains where the local averages are acting. As a result, the larger s, the sooner this redundancy will appear and the more unstable the process.

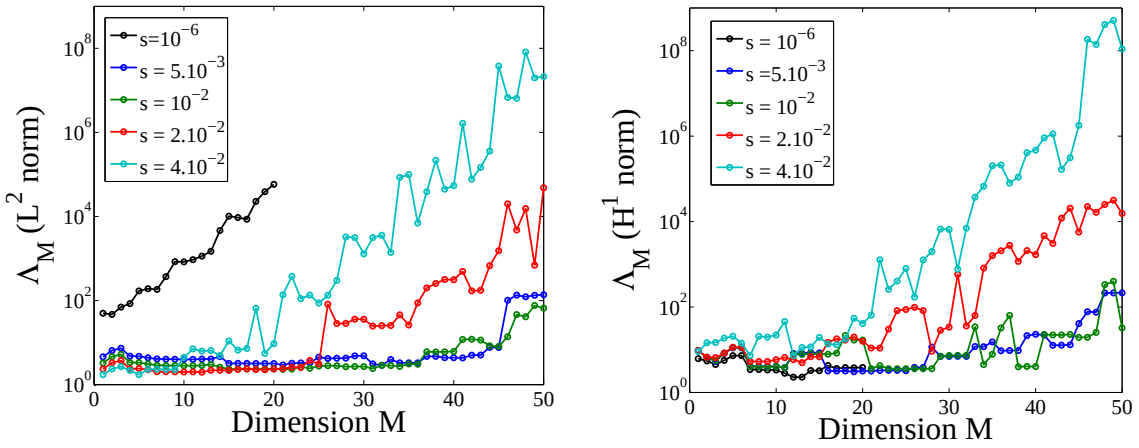

(a) L^2 norm. **(b)** H^1 norm.

Figure 3: Impact on Λ_M of the parameter s of the linear functionals.

It is also important to understand the behavior when the parameter s tends to zero. In this case, the linear functionals tend to Dirac masses, that are elements of H^{-1} but not of L^2. Hence, in the limit $s = 0$, the definition of the space W_M will be possible in H^1 but not in L^2 because the problem:

$$\begin{cases} \text{Find } w_i \in \mathcal{X} \text{ such that:} \\ \sigma_i(\varphi) = (w_i, \varphi)_{\mathcal{X}} = \delta_{x_i}(\varphi), \quad \forall \varphi \in \mathcal{X} \end{cases} \tag{28}$$

is well-defined in H^1 and not in L^2. This observation helps to understand first of all why Λ_1 remains roughly constant in H^1 as s decreases whereas it behaves as $s^{-1/2}$ in the L^2 norm (see figure 4). Indeed, in the H^1 case, we have the inequality

$$\frac{\|\mathcal{J}_1[\varphi]\|_{H^1(\Omega)}}{\|\varphi\|_{H^1(\Omega)}} = |\sigma_1(\varphi)| \frac{\|q_1\|_{H^1(\Omega)}}{\|\varphi\|_{H^1(\Omega)}} \leq \|\varphi\|_{L^\infty(\Omega)} \frac{\|q_1\|_{H^1(\Omega)}}{\|\varphi\|_{H^1(\Omega)}}, \quad \forall \varphi \in H^1(\Omega),$$

which is bounded for any $s \in \mathbb{R}_+$. However, in the case of $L^2(\Omega)$, it can be inferred that

$$\frac{\|\mathcal{J}_1[\varphi]\|_{L^2(\Omega)}}{\|\varphi\|_{L^2(\Omega)}} = |\sigma_1(\varphi)| \frac{\|q_1\|_{L^2(\Omega)}}{\|\varphi\|_{L^2(\Omega)}} \leq \frac{\|m_{1,s}\|_{L^2(\Omega)}}{\|m_{1,s}\|_{L^1(\Omega)}} \|q_1\|_{L^2(\Omega)}, \quad \forall \varphi \in H^1(\Omega)$$

where we have applied the Cauchy-Schwarz inequality to $|\sigma_1(\varphi)|$. A simple change of variable $u = \dfrac{x - x_1}{s}$ in the

evaluation of $\frac{\|m_{1,s}\|_{L^2(\Omega)}}{\|m_{1,s}\|_{L^1(\Omega)}}$ leads to the bound

$$\frac{\|\mathcal{J}_1[\varphi]\|_{L^2(\Omega)}}{\|\varphi\|_{L^2(\Omega)}} \leq C\|q_1\|_{L^2(\Omega)} s^{-1/2}, \quad \forall \varphi \in L^2(\Omega), \tag{29}$$

where

$$C = \frac{\int_\Omega e^{-u^2} du}{\int_\Omega e^{-u^2/2} du}.$$

In figure 4, note that for values $s \leq 10^{-4}$, the behavior of Λ_1 no longer follows $s^{-1/2}$ but this is due to computer limitations. Indeed, the computations have been carried out with a maximum number of 10^4 degrees of freedom in the $\mathbb{P}_1$ approximation because of memory storage issues. As a result, for $s \leq 10^{-4}$, we no longer capture enough information with this finite element precision.

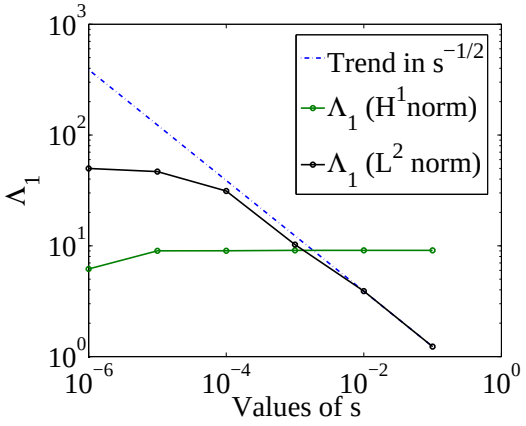

Figure 4: Behavior of Λ_1 as a function of s (H^1 and L^2 norms). Remark: the scale of the figure is log-log.

As a consequence of the diverging behavior of Λ_1 in L^2 as the parameter s decreases, it is reasonable to expect that the sequence (Λ_M) quickly diverges as $s \to 0$ in L^2 but that it remains bounded in H^1. This behavior is indeed illustrated in figures 3a and 3b through the example of $s = 10^{-6}$, in which it is possible to observe the phenomenon.

5. Application of GEIM to the real-time monitoring of a physical experiment

The main purpose of this section is to illustrate that GEIM can be used as a tool for the real-time monitoring of a physical or industrial process. This will be done by combining mathematical models (a parameter dependent PDE) with measurements from the experiment.

5.1. The general method

Let us assume that we want to monitor in real time a field u_{true} appearing as an input for some quantities of interest in a given experiment that involves sensor measurements. We assume that the conditions of the experiment are described by a vector of parameters $\mu_{\text{true}} \in E$, where E is a compact set of $\mathbb{R}^p$, and that u_{true} is the solution of a parameter dependent PDE

$$D_\mu u = g_\mu \quad \mu \in E \tag{30}$$

when $\mu = \mu_{\text{true}}$ (in other words $u_{\text{true}} = u_{\mu_{\text{true}}}$). The vector μ_{true} will be unknown in general so the computation of u_{true} cannot be done by traditional discretization techniques like finite elements. Besides, even if μ_{true} was known,

its computation could not be performed in real-time with classical techniques. For all these reasons, we propose to compute the generalized interpolant $\mathcal{J}_M[u_{\text{true}}]$ as an approximation of u_{true} that can be derived in real time and that does not sacrifice much on the accuracy of the approximation.

Such an approximation requires that the set of solutions $\{u_\mu, \forall \mu \in E\}$ is included in some compact set F of $\mathcal{X}$ that is of small Kolmogorov n-width in $\mathcal{X}$ ([12]). A dictionary $\Sigma \subset \mathcal{L}(\mathcal{X})$ is also required, but note that the sensors of the experiment can mathematically be modelled by elements of $\mathcal{L}(\mathcal{X})$. We will therefore assume that we have a dictionary composed of the linear functionals representing each one of the sensors.

Since we need to define the generalized interpolating spaces $X_M = \text{span}\{q_1, \dots, q_M\}$ together with the suitable interpolating linear functionals $\{\sigma_1, \dots, \sigma_M\}$, a greedy algorithm has to be performed beforehand and therefore the computation of $\mathcal{J}_M[u_{\text{true}}]$ is divided into two steps:

- In an *offline phase* (i.e. before the experiment takes place):
  - We define a finite subset $\mathcal{S}_F = \{u(\mu, .), \mu \in \Xi_\mu \subset E\} \subset F$ and solve (30) for each element of $\mathcal{S}_F$ with an accurate enough discretization strategy. This can be done with traditional approximation tools like, e.g., finite elements or a reduced basis strategy.
  - Following the steps of algorithm 1, a greedy algorithm over the set $\mathcal{S}_F$ is performed to build an M-dimensional reduced basis $X_M = \text{span}\{q_j \in F, j \in [1, M]\}$ together with the suitable linear functionals $\{\sigma_1, \dots, \sigma_M\}$. The selection of the linear functionals means that, among all the sensors in the experiment that constitute our dictionary Σ, we select the M most suitable according to the greedy criterion.
- In an *online phase* (i.e. when the experiment is running), we collect in real time the measurements

$$\{\sigma_1(u_{\mu_{\text{true}}}), \dots, \sigma_M(u_{\mu_{\text{true}}})\}$$

  from the M selected sensors. The generalized interpolant $\mathcal{J}_M[u_{\mu_{\text{true}}}]$ can then be computed following formula (3). It has been observed so far (see the numerical example below and [1]) that the interpolation error decreases very quickly as the dimension M increases and therefore relatively small values of M are required to reach a good accuracy in the approximation of $u_{\mu_{\text{true}}}$ by $\mathcal{J}_M[u_{\mu_{\text{true}}}]$. Thanks to this, the computation of $\mathcal{J}_M[u_{\mu_{\text{true}}}]$ can be performed in real-time (or almost).

Remark 5.1. *Note that our strategy supposes that the physical experiment u_{true} is perfectly described by the solution u_μ of (30) when $\mu = \mu_{true}$. This is a very strong hypothesis because the model might not perfectly describe the experiment under consideration. Besides, it is here assumed that there is no noise in the measurements, which is also a strong assumption. In [1], some preliminary analysis has been presented to take into account the presence of noise in the measurements. Regarding the model bias, in the recent works of [18, 19], the authors are able to take it into account under several hypothesis in the so called "Parametrized-Background Data-Weak Formulation" for variational data assimilation. In fact, GEIM is a particular instance of this method for the case (with the notations of [19]) $N = M$ and this latter choice is appropriate for situations in which the bias is small.*

Remark 5.2. *In the strategy proposed in this section, sensor measurements are incorporated in the interpolation procedure through the space W_M (which is spanned by the Riesz representations of the linear functionals of the sensors). In the reference [20], one can find an early work in oceanography in which data assimilation is also incorporated through the construction of the space W_M. However, in the case of [20], no a priori error analysis was provided in the computational procedure that was proposed.*

5.2. A numerical application involving the Stokes equation

We are going to illustrate the procedure in the case where the experiment corresponds to a lid-driven cavity problem that takes place in the spatial domain $\Omega = [0; 1] \times [0; 1] \subset \mathbb{R}^2$. We consider two parameters $\boldsymbol{\mu} = (\mu_1, \mu_2) \in [1; 8] \times [1; 8]$ such that, for a given μ, the parametrized PDE reads:

$$
\begin{cases}
\text{Find the solution } (\boldsymbol{u}_\mu, p_\mu) \in \left(H^1(\Omega)\right)^2 \times L^2(\Omega) \text{ of :} \\
-\Delta \boldsymbol{u}_\mu + \mathbf{grad}(p_\mu) = \mathbf{f}_\mu, \text{ in } \Omega \\
\text{div}(\mathbf{u}_\mu) = 0, \text{ in } \Omega \\
\mathbf{u}_\mu = \begin{pmatrix} x(1-x) \\ 0 \end{pmatrix}, \text{ on } \Gamma_1 \\
\mathbf{u}_\mu = \mathbf{0}, \text{ on } \partial\Omega \setminus \Gamma_1
\end{cases}
\tag{31}
$$

where the forcing term $\mathbf{f}_\mu = \begin{pmatrix} 100\sin(\mu_1 \Pi y) \\ -100\sin\left(\mu_2 \Pi \frac{1-x}{2}\right) \end{pmatrix}$ and $\Gamma_1 = \{x \in [0;1],\ y = 1\}$. Two examples of solutions are provided on figures 5 and 6.

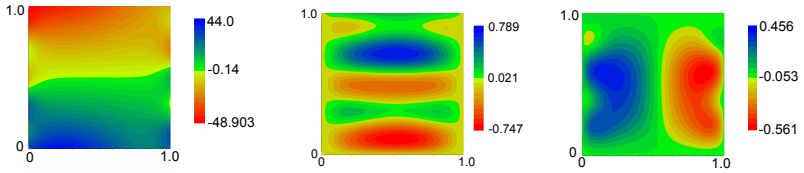

Figure 5: From left to right: pressure, horizontal and vertical velocity solutions for the parameter $\boldsymbol{\mu} = (5; 1)$.

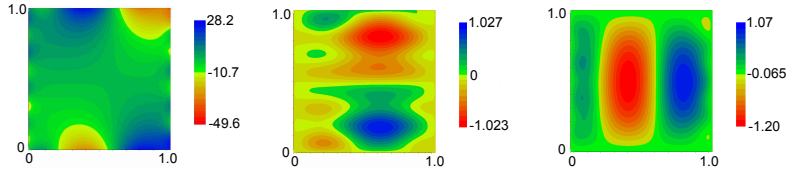

Figure 6: From left to right: pressure, horizontal and vertical velocity solutions for the parameter $\boldsymbol{\mu} = (8; 5)$.

We assume that:

- The set of solutions $\{(\mathbf{u}, p)(\mu),\ \forall \mu\} \subset F$ and F is of small Kolmogorov n-width in $\left(H^1(\Omega)\right)^2 \times L^2(\Omega)$. This assumption is made *a priori* and will be verified *a posteriori* in a convergence study of the interpolation errors.
- we have velocity and pressure sensors at our disposal which mathematically means that we have:
  - a dictionary for the velocity: $\Sigma^{\mathbf{u}} = \{\sigma^{\mathbf{u}}\} \subset \mathcal{L}(H^1(\Omega)^2)$
  - a dictionary for the pressure: $\Sigma^p = \{\sigma^p\} \subset \mathcal{L}(L^2(\Omega))$

In our numerical example, the linear functionals that have been used consist on local averages of the same form as (26) and (27) but adapted to the 2D case. The parameter s has been fixed to $s = 10^{-3}$ and we will have $N_{sensor} = 100$ sensors for the pressure and other $N_{sensor} = 100$ sensors for the velocity. The centers of these local averages are located on a 10×10 equispaced grid of Ω.

Given an experiment corresponding to the vector of parameters μ_{exp}, we are going to — quickly and accurately— approximate in Ω the vectorial field $(\mathbf{u}, p)(\mu_{\text{exp}})$ by its generalized interpolant $\mathcal{J}_M\left[(\mathbf{u}, p)(\mu_{\text{exp}})\right]$ thanks to the only knowledge of measurements from sensors. Because we are facing here the reconstruction of a vectorial field, several potential input from $(\mathbf{u}, p)(\mu)$ can be proposed. In the present paper, three classes of them will be considered. They will all fulfill the divergence-free condition for the velocity interpolant $\text{div}\left(\mathcal{J}_M\left[\mathbf{u}(\mu)\right]\right) = 0$.

Reconstruction 1: Independent treatment of $u(\mu)$ and $p(\mu)$.
The first possibility consists in considering $(\mathbf{u}, p)(\mu)$ not as a vectorial field but as two independent fields $\mathbf{u}(\mu)$ and $p(\mu)$

to interpolate independently with velocity measurements for $\mathbf{u}(\mu)$ and pressure measurements for $p(\mu)$. In other words, the generalized interpolant is defined in this case as $\mathcal{J}_{M_\mathbf{u},M_p}[(\mathbf{u},p)(\mu)] = \left(\mathcal{J}^{\mathbf{u}}_{M_\mathbf{u}}[\mathbf{u}(\mu)];\mathcal{J}^{p}_{M_p}[p(\mu)]\right)$. This requires the offline computation of two greedy algorithms: one for the velocity and another for the pressure. Each one respectively provides:

- a velocity basis $\{\mathbf{u}(\mu_i)\}_{i=1}^{M_\mathbf{u}}$ and a set of $M_\mathbf{u}$ velocity sensors $\{\sigma^{\mathbf{u}}_i\}_{i=1}^{M_\mathbf{u}}$ chosen among the dictionary $\Sigma^{\mathbf{u}}$. The interpolant for the velocity will be $\mathcal{J}^{\mathbf{u}}_{M_\mathbf{u}}[\mathbf{u}(\mu)] = \sum_{i=1}^{M_\mathbf{u}} \alpha_i \mathbf{u}(\mu_i)$ where the α_i are given by the interpolating conditions $\sigma^{\mathbf{u}}_i\left(\mathcal{J}^{\mathbf{u}}_{M_\mathbf{u}}[\mathbf{u}(\mu)]\right) = \sigma^{\mathbf{u}}_i\left(\mathbf{u}(\mu)\right),\ \forall i \in \{1,\dots,M_\mathbf{u}\}$.
- a pressure basis $\{p(\mu_j)\}_{j=1}^{M_p}$ and a set of pressure sensors $\{\sigma^{p}_j\}_{j=1}^{M_p}$ chosen among Σ^p. The interpolant for the pressure will be $\mathcal{J}^{p}_{M}[p(\mu)] = \sum_{j=1}^{M_p} \gamma_j p(\mu_j)$ where the γ_j are given by the interpolating conditions $\sigma^{p}_j\left(\mathcal{J}^{p}_{M_p}[p(\mu)]\right) = \sigma^{p}_j\left(p(\mu)\right),\ \forall j \in \{1,\dots,M_p\}$.

Note that in this approximation, the construction of $\mathcal{J}_{M_\mathbf{u},M_p}[(\mathbf{u},p)(\mu)]$ involves M_p pressure sensors and $M_\mathbf{u}$ velocity sensors, i.e. $M_p + M_\mathbf{u}$ coefficients. In figure 7, we have represented the locations of the sensors in the order given by the greedy algorithm.

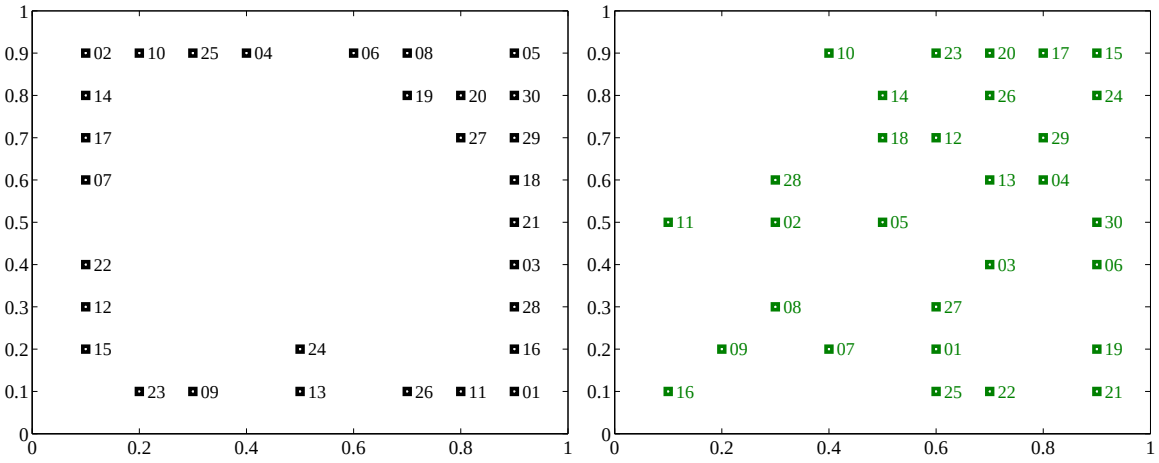

(a) Pressure sensors **(b)** Velocity sensors

Figure 7: Locations of the sensors for reconstruction 1.

The performances of the method are plotted in figure 8 where a numerical estimation of the behavior of the interpolating errors for the reconstruction of u and p have been represented. These values have been obtained by the interpolation of 196 configurations coming from different parameter values μ_i following formula:

$$\begin{cases} e^{p}_{M_p} = \max\limits_{i\in\{1,\dots,196\}} \dfrac{\|p(\mu_i) - \mathcal{J}^{p}_{M_p}[p(\mu_i)]\|_{L^2(\Omega)}}{\|p(\mu_i)\|_{L^2(\Omega)}} \\ e^{\mathbf{u}}_{M_\mathbf{u}} = \max\limits_{i\in\{1,\dots,196\}} \dfrac{\|\mathbf{u}(\mu_i) - \mathcal{J}^{\mathbf{u}}_{M_\mathbf{u}}[\mathbf{u}(\mu_i)]\|_{H^1(\Omega)^2}}{\|\mathbf{u}(\mu_i)\|_{H^1(\Omega)^2}}. \end{cases} \tag{32}$$

In this figure, we can observe the convergence of the interpolation errors for both the velocity and pressure fields. After a preasymptotic stage for interpolating spaces of small dimension, an exponential convergence of the error is

observed. After about dimension $M = 25$, the error stagnates due to the fact that we have reached the finite element accuracy used for the computation of the offline snapshots. The computation of the Lebesgue constants

$$\Lambda^p_{M_p} := \sup_{p\in L^2(\Omega)} \frac{\|\mathcal{J}^p_{M_p}(p)\|_{L^2(\Omega)}}{\|p\|_{L^2(\Omega)}}, \quad \Lambda^{\mathbf{u}}_{M_{\mathbf{u}}} = \sup_{\boldsymbol{u}\in H^1(\Omega)^2} \frac{\|\mathcal{J}^{\mathbf{u}}_{M_{\mathbf{u}}}(\mathbf{u})\|_{H^1(\Omega)^2}}{\|\mathbf{u}\|_{H^1(\Omega)^2}} \tag{33}$$

has also been performed following formula (15). Its behavior seems linear with the dimension of interpolation and is therefore far from the crude theoretical upper bound given in formula (8). From the results presented in section 4, an idea to improve the behavior of the Lebesgue constant could be to consider a smaller value for s. However, in the present context, we have not sought the optimization of (Λ_M) as a function of the parameter s because, in a real case, the linear functionals are fixed by the filter characteristics of the sensors involved in the experiment.

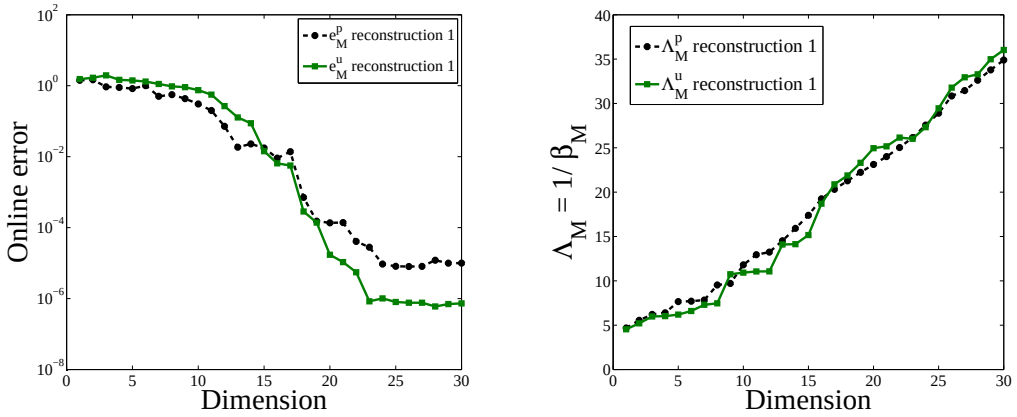

Figure 8: Reconstruction 1: A numerical estimation of the behavior of the interpolation error (left) and the Lebesgue constant (right) as a function of the dimension of the interpolating spaces X_M

Reconstructions 2 and 3: Vectorial treatment for $\mathbf{u}(\mu)$ and $p(\mu)$.
An alternative to the first reconstruction is to consider $(\mathbf{u}, p)(\mu)$ as a vectorial field and define its generalized interpolant as $\mathcal{J}_M[(\mathbf{u}, p)(\mu)] := \sum_{i=1}^{M} \gamma_i(\mathbf{u}, p)(\mu_i)$, where now only M coefficients γ_i are involved. The joint basis $\{(\mathbf{u}, p)(\mu_i)\}_{i=1}^M$ is provided by a greedy algorithm in the online stage together with a set of M linear functionals $\{\sigma_i^{(\mathbf{u},p)}\}_{i=1}^M$. Each of these linear functionals involve pressure and velocity measurements at a given spatial location and are defined as $\sigma_i^{(\mathbf{u},p)} := \sigma_i^{\mathbf{u}}(\mathbf{u}) + \sigma_i^p(p)$. The interpolating conditions for the inference of the coefficients γ_i are now the following:

$$\sigma_i^{(\mathbf{u},p)}\Big((\mathbf{u}, p)(\mu)\Big) = \sigma_i^{(\mathbf{u},p)}\Big(\mathcal{J}_M[(\mathbf{u}, p)(\mu)]\Big) = \sum_{j=1}^{M} \gamma_j \sigma_i^{(\mathbf{u},p)}\Big((\mathbf{u}, p)(\mu_j)\Big), \ \forall i \in \{1, \ldots, M\}, \tag{34}$$

Notice that this definition of the linear functionals $\sigma^{(\mathbf{u},p)}$ can involve both velocity and pressure measurements or can take into account velocity or pressure measurements only by setting $\sigma^{\mathbf{u}} = 0$ or $\sigma^p = 0$. We have explored this flexibility in the following two reconstructions where we have compared:

- the interpolation of the pressure and velocity fields with pressure and velocity measurements: $\sigma_i^{(\mathbf{u},p)} := \sigma_i^{\mathbf{u}}(\mathbf{u}) + \sigma_i^p(p)$ (reconstruction 2).
- the interpolation of the pressure and velocity fields with pressure measurements only: $\sigma_i^{(\mathbf{u},p)} := \sigma_i^p(p)$. In other words, we are here studying if a velocity field can efficiently be reconstructed with the only knowledge of pressure measurements (reconstruction 3).

The sensor locations provided by the greedy algorithm are shown in figure and 9 and the results are summarized in figures 10 where an estimation of the interpolation error is plotted according to formula (35).

$$e_M^{(\mathbf{u},p)} = \max_{i\in\{1,\dots,196\}} \frac{\|(\mathbf{u},p)(\mu_i) - \mathcal{J}_M^{(\mathbf{u},p)}\left[(\mathbf{u},p)(\mu_i)\right]\|_{H^1(\Omega)^2\times L^2(\Omega)}}{\|(\mathbf{u},p)(\mu_i)\|_{H^1(\Omega)^2\times L^2(\Omega)}}. \tag{35}$$

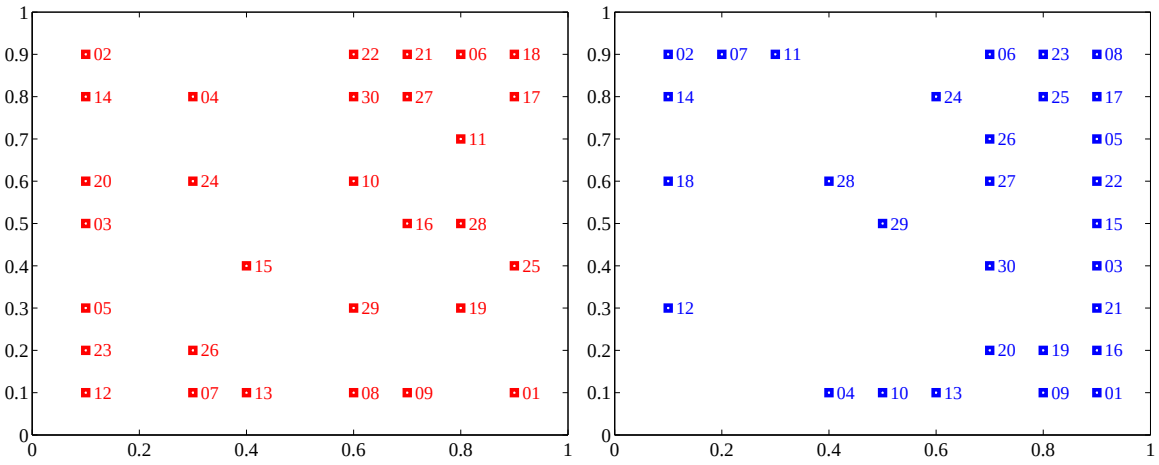

(a) Reconstruction 2 **(b)** Reconstruction 3

Figure 9: Locations of the sensors for reconstructions 2 and 3.

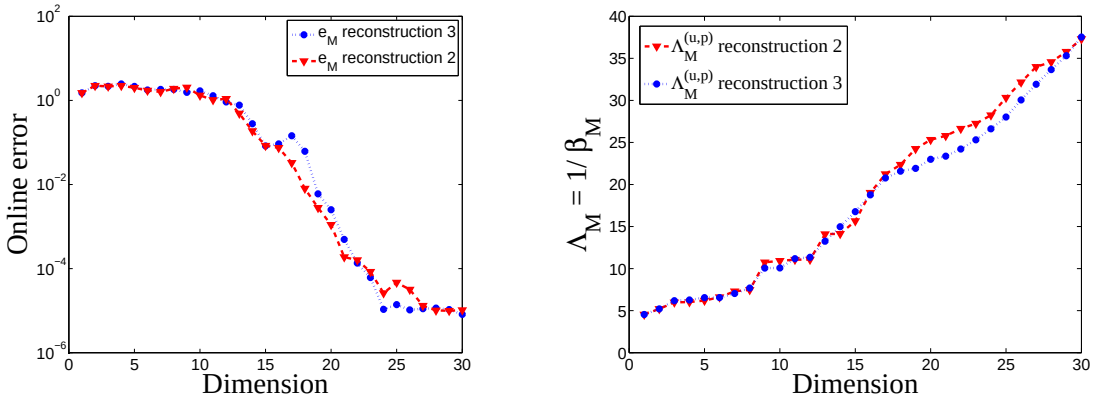

Figure 10: Reconstructions 2 and 3: A numerical estimation of the behavior of the interpolation error (left) and the Lebesgue constant (right) as a function of the dimension of the interpolating spaces X_M.

The interpolating error of the two types of reconstructions presents a very similar decay behavior in both cases and the convergence is also very similar to reconstruction 1. The most interesting consequence of this is that the velocity can efficiently be reconstructed with only pressure measurements. This result cannot probably be generalized to all

types of situations but it proves that in some cases like the current one there is some redundancy in the datas and that, in this precise problem, there is no need in having velocity measurements in order to obtain a good accuracy in the approximation of the velocity field.

The Lebesgue constant

$$\Lambda_M^{(\boldsymbol{u},p)} = \sup_{(\boldsymbol{u},p)\in H^1(\Omega)^2\times L^2(\Omega)} \frac{\|\mathcal{J}_M^{(\mathbf{u},p)}(\mathbf{u},p)\|_{H^1(\Omega)^2\times L^2(\Omega)}}{\|(\mathbf{u},p)\|_{H^1(\Omega)^2\times L^2(\Omega)}} \tag{36}$$

has also been computed for reconstructions 2 and 3 as is shown in figure 10. Once again, the behavior is linear which is a moderate growth rate.

6. Conclusion and perspectives

After revisiting the foundations of GEIM for Banach spaces, the present work has focused on understanding the stability of the process and a relation between Λ_M and an inf-sup problem has been established in the particular case of Hilbert spaces. An interpretation of the generalized interpolant as an oblique projection has also been presented in that case. The derived formula for Λ_M has also allowed us to notice that the Greedy algorithm optimizes in some sense the Lebesgue constant.

A first analysis about the impact of the dictionary of linear functionals Σ on the Lebesgue constant has also been presented through a numerical test case. Furthermore, for a given dictionary Σ, the Lebesgue constant depends on the norm of the ambient space $\mathcal{X}$ (see formula (7)). A comparison of the behavior of (Λ_M) when $\mathcal{X} = L^2$ or H^1 has been provided in the case of a dictionary composed of simple local averages.

Beyond these results, there are still plenty of challenging theoretical open questions. Among the most important we mention:

- the obtention (if possible) of a general theory on the impact of Σ on the behavior of (Λ_M) and of a tighter upper bound than the one presented in (8).
- When the number of involved parameters is very large, how to deal with the offline phase in a reasonable time?
- How to include the bias between u_{true} and the manifold of solutions of our parameter dependent PDE? The works of [18] will probably be helpful to carry out this task.
- How to deal with noisy measurements? One can find some preliminary ideas in [1] and the works of [21].

Furthermore, the recent results of [12] lead us to think that it would be interesting to explore non-linear inputs of the form

$$\sigma\left(t(\varphi)\right),$$

where $\sigma \in \mathcal{L}(\mathcal{X})$, $t : \mathcal{X} \to \mathcal{X}$ is a non linear mapping and φ is an element of a compact set of small Kolmogorov n-width in $\mathcal{X}$. In an ongoing work, we are exploring this idea in the case of the Navier-Stokes equations.

On a second part of the paper, we have illustrated one of the most straightforward practical applications of GEIM that consists in monitoring in real-time a process. The idea is that GEIM could reconstruct in real-time physical quantities in the whole domain of an experiment by combining the real-time acquisition of measurements from sensors with mathematical models (parameter dependent PDE's).

This scheme has been applied to an example dealing with a parametrized lid-driven Stokes equation. The example shows a fast decrease in the interpolation error, which confirms that it is feasible to use GEIM to monitor experiments in real-time in cases where $d_n(F,\mathcal{X})$ is small enough (i.e. when the experiment is simple enough). The behavior of the Lebesgue constant seems to be linear and seems to be in accordance with previous works for the classical EIM (see [4]). The linear increase is far from the theoretical exponential upper bound of (8) and suggests that the bound might not be optimal in sets F of small Kolmogorov n-width. In the example, two types of sensors have been used (of pressure and velocity) and the idea of introducing different types of sensors could be extended to make more adequate distinctions among them.

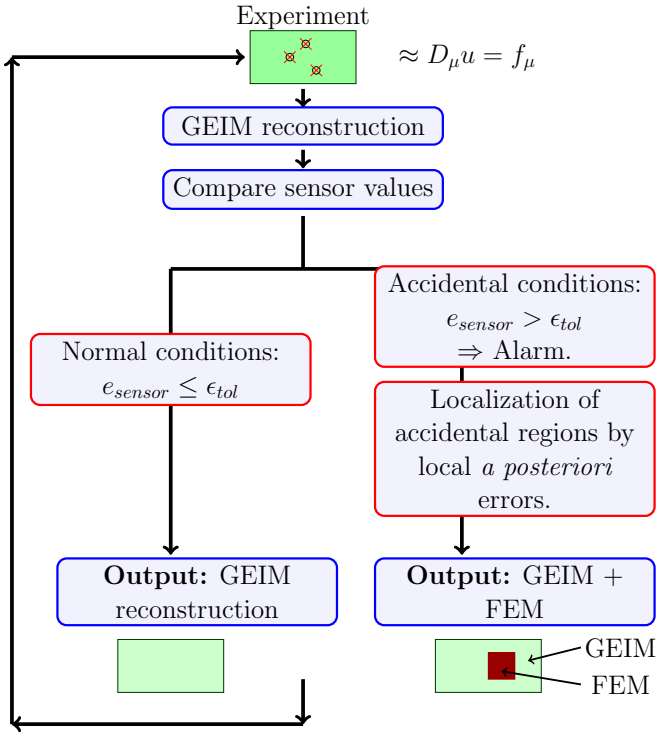

Figure 11: A tool to supervise in real-time the safety of an experiment.

By taking this method as a starting point, GEIM could be used to devise a more complete tool capable of supervising the safety of processes (see figure 11). The idea would be the following: given an experiment, we start by reconstructing it by GEIM. Let us assume that we have, e.g., $2M$ sensors at our disposal but that GEIM only needs the information of M of them to provide the reconstruction with the desired accuracy. We can then numerically compute the output of the rest of the sensors by using the generalized interpolant and compare this to the values coming from the experiment. If the values differ too much from each other, then we consider that an abnormal event has occurred in the experiment and an alarm can be launched to inform of the incident.

Further than this alarm information, we can seek to provide an accurate enough reconstruction of the solution during the incident by using the following strategy: through the computation of an posteriori error estimator in the regions where the sensor measurements are not in accordance, we could imagine to localize the spatial region(s) where the reconstruction is no longer accurate. The domain could then be split into:

- a subdomain with small Kolmogorov n-width where the reconstruction by GEIM is still accurate enough.
- a subdomain with big Kolmogorov n-width where the accident is located and GEIM is no longer accurate. The domain is computed by traditional discretization techniques such as finite elements complemented with Dirichlet boundary conditions from the GEIM reconstruction.

Under the hypothesis that the accidental subdomain is small, the reconstruction could still be done in a relatively quick time, preserving the real-time aspect of our device. The feasibility of decomposing the domain and coupling GEIM with other approximations has been explored in [1] in a simple Laplace problem.

Last but not least, it would also be interesting to explore the robustness of the method in cases where one or several sensors involved in the GEIM reconstruction fail.

Appendix A.

Corollary Appendix A.1. *Let $\mathcal{X}$ be a Hilbert space and E, F two subspaces of $\mathcal{X}$. Then, $\beta_{E,F} = \beta_{F^\perp,E^\perp}$, where:*

$$\beta_{E,F} \equiv \inf_{\substack{e\in E\\ \|e\|=1}} \sup_{\substack{f\in F\\ \|f\|=1}} (e,f) \tag{A.1}$$

$$\beta_{F^\perp,E^\perp} \equiv \inf_{\substack{f\in F^\perp\\ \|f\|=1}} \sup_{\substack{e\in E^\perp\\ \|e\|=1}} (e,f). \tag{A.2}$$

Proof. Given $e \in \mathcal{X}$ of norm unity, we introduce f_e^* as

$$f_e^* = \arg \sup_{\substack{g\in F\\ \|g\|=1}} (e,g).$$

We can then show from optimality that $(e,h) = 0$ for all h in $\{q \in F \,|\, (q, f_e^*) = 0\}$ and hence

$$e = \lambda f_e^* + \varepsilon \tag{A.3}$$

for some $\lambda \in \mathcal{R}$ and $\varepsilon \in F^\perp$ such that $\lambda^2 + \|\varepsilon\|^2 = 1$ (from our normalization and orthogonality). We then deduce from (A.3), orthogonality, and Cauchy-Schwarz that

$$\sup_{\substack{p\in F\\ \|p\|=1}} (e,p) = \lambda$$

and

$$\sup_{\substack{p\in F^\perp\\ \|p\|=1}} (e,p) = \|\varepsilon\|.$$

Hence,

$$\Big(\sup_{\substack{p\in F\\ \|p\|=1}} (e,p)\Big)^2 + \Big(\sup_{\substack{p\in F^\perp\\ \|p\|=1}} (e,p)\Big)^2 = 1 \tag{A.4}$$

thanks to our normalization.

We may now note from (A.1) and (A.4) that

$$\begin{aligned}
\beta_{E,F} &= \inf_{\substack{e\in E\\ \|e\|=1}} \sqrt{1 - \Big(\sup_{\substack{p\in F^\perp\\ \|p\|=1}} (e,p)\Big)^2} \\
&= \sqrt{1 - \Big(\sup_{\substack{e\in E\\ \|e\|=1}} \sup_{\substack{p\in F^\perp\\ \|p\|=1}} (e,p)\Big)^2} \\
&= \sqrt{1 - \Big(\sup_{\substack{p\in F^\perp\\ \|p\|=1}} \sup_{\substack{e\in E\\ \|e\|=1}} (e,p)\Big)^2}
\end{aligned} \tag{A.5}$$

as we can exchange the two supremizer operations.

Finally, we define a second inf-sup constant,

$$\beta_{F^\perp,E^\perp} \equiv \inf_{\substack{f\in F^\perp\\ \|f\|=1}} \sup_{\substack{e\in E^\perp\\ \|e\|=1}} (e,f). \tag{A.6}$$

We can repeat the procedure above — E goes to $F^\perp$ and F goes to $E^\perp$ — to find

$$\beta_{F^\perp,E^\perp} = \sqrt{1 - \Big(\sup_{\substack{p\in F^\perp\\ \|p\|=1}} \sup_{\substack{e\in (E^\perp)^\perp\\ \|e\|=1}} (e,p)\Big)^2}, \tag{A.7}$$

and hence conclude from (A.5) and (A.7) that

$$\beta_{E,F} = \beta_{F^\perp,E^\perp}$$

since $(E^\perp)^\perp = E$. □

Appendix B.

We propose here a practical method for the computation of

$$\sup_{\varphi\in\mathcal{X}}\frac{\|\mathcal{J}_M[\varphi]\|_{\mathcal{X}}}{\|\varphi\|_{\mathcal{X}}}. \tag{B.1}$$

The strategy consists in using a finite element Galerkin projection as an approximation of the elements of $\mathcal{X}$. We therefore propose to compute

$$\max_{\varphi\in V_h^k}\frac{\|\mathcal{J}_M[\varphi]\|_{V_h^k}}{\|\varphi\|_{V_h^k}}$$

as a surrogate of (B.1), where V_h^k is the classical continuous finite element approximating space of mesh size h that involves piece-wise $\mathbb{P}_k$ polynomials. Let $\mathcal{B} = \text{span}\{b_1, \dots, b_{\mathcal{N}}\}$ be a basis of V_h^k and let M be the $\mathcal{N}\times\mathcal{N}$ mass matrix of entries $M_{i,j} = (b_i, b_j)_{\mathcal{X}}$, $1 \le i, j \le \mathcal{N}$. For any $\varphi \in V_h^k$, let

$$\boldsymbol{\varphi} = (\varphi_1, \dots, \varphi_{\mathcal{N}})^T \tag{B.2}$$

be the vector of coordinates of φ in the basis $\mathcal{B}$. In coherence with these notations, for any $1 \le i \le M$, the vectors

$$\boldsymbol{q_i} = (q_{1,i}, \dots, q_{\mathcal{N},i})^T \quad \text{and} \quad \boldsymbol{w_i} = (w_{1,i}, \dots, w_{\mathcal{N},i})^T \tag{B.3}$$

will respectively denote the Galerkin projections onto V_h^k of the interpolating basis functions $q_i \in \mathcal{X}$ and of the Riesz representation of the i-th linear functional, σ_i. Furthermore, let Q^M be the $\mathcal{N}\times M$ matrix such that

$$Q^M = [\boldsymbol{q_1}, \dots, \boldsymbol{q_M}],$$

and let C^M be the $M\times\mathcal{N}$ matrix such that:

$$C^M_{i,j} = \sigma_i(b_j) = (w_i, b_j)_{\mathcal{X}}, \quad \forall 1 \le i \le M,\ 1 \le j \le \mathcal{N}.$$

Finally, we recall that B^M is the $M\times M$ matrix defined in section 1 whose entries are

$$B^M_{i,j} = \sigma_i(q_j) = (w_i, q_j)_{\mathcal{X}}, \quad \forall 1 \le i \le M,\ 1 \le j \le M.$$

An approximation of the entries of B^M and C^M can easily be computed by using the finite element Galerkin projections of the involved functions:

$$\begin{cases} C^M_{i,j} \approx \boldsymbol{w_i}^T M \boldsymbol{b_j}, & \forall 1 \le i \le M,\ 1 \le j \le \mathcal{N} \\ B^M_{i,j} \approx \boldsymbol{w_i}^T M \boldsymbol{q_j}, & \forall 1 \le i \le M,\ 1 \le j \le M. \end{cases}$$

With these notations, we can easily prove

Lemma Appendix B.1. *Let T be the $\mathcal{N}\times\mathcal{N}$ symmetric positive definite matrix:*

$$T := \left(Q^M(B^M)^{-1}C^M\right)^T M \left(Q^M(B^M)^{-1}C^M\right),$$

and let $\lambda_{\max}(T)$ be the largest eigenvalue of the generalized eigenvalue problem

$$\begin{cases} \text{Find } (\lambda, x) \in \mathbb{R}\times\mathbb{R}^{\mathcal{N}} \text{ such that:} \\ Tx = \lambda M x. \end{cases} \tag{B.4}$$

Then:

$$\max_{\varphi\in V_h^k}\frac{\|\mathcal{J}_M[\varphi]\|_{\mathcal{X}}}{\|\varphi\|_{\mathcal{X}}} = \sqrt{\lambda_{\max}}. \tag{B.5}$$

Proof. For any $\varphi \in V_h^k$ and any $1 \leq i \leq M$:

$$\sigma_i(\varphi) = \sum_{j=1}^{\mathcal{N}} \varphi_j \sigma_i(b_j) = \boldsymbol{e_i}^T C^M \boldsymbol{\varphi},$$

where $\boldsymbol{e_i}$ is the i-th canonical vector of dimension M. Furthermore, if

$$\mathcal{J}_M[\varphi] = \sum_{i=1}^{M} \alpha_i^M(\varphi) q_i \tag{B.6}$$

is the generalized interpolant of φ in dimension M, we have:

$$\sigma_i\left(\mathcal{J}_M[\varphi]\right) = \boldsymbol{e_i}^T B^M \boldsymbol{\alpha}, \quad \forall 1 \leq i \leq M,$$

where $\boldsymbol{\alpha} = \left(\alpha_1^M(\varphi), \ldots, \alpha_M^M(\varphi)\right)^T$. From the interpolation property stated in (3), it follows that

$$\boldsymbol{\alpha} = \left(B^M\right)^{-1} C^M \boldsymbol{\varphi}.$$

Then, the finite element Galerkin projection of the interpolant of (B.6) can be expressed as:

$$\mathcal{J}_M[\varphi] \approx Q^M \boldsymbol{\alpha} = Q^M \left(B^M\right)^{-1} C^M \boldsymbol{\varphi}.$$

Hence,

$$\begin{aligned} \max_{\varphi \in V_h^k} \frac{\|\mathcal{J}_M[\varphi]\|_X}{\|\varphi\|_X} &= \left(\max_{\varphi \in \mathbb{R}^{\mathcal{N}}} \frac{\boldsymbol{\varphi}^T \left(Q^M (B^M)^{-1} C^M\right)^T M \left(Q^M (B^M)^{-1} C^M\right) \boldsymbol{\varphi}}{\boldsymbol{\varphi}^T M \boldsymbol{\varphi}} \right)^{1/2} \\ &= \sqrt{\lambda_{\max}(T)}. \end{aligned}$$

□

Remark Appendix B.2. *The computation of $\Lambda_{\max}$ can easily be performed by, e.g., the power method scheme applied to the matrix T. However, note that the evaluation of Λ_M with formula (B.5) requires the construction of T, which is a large dense matrix of dimension $\mathcal{N} \times \mathcal{N}$. In cases where the storage of T is no longer possible, the Lebesgue constant can still be computed with formula (24), whose evaluation requires the construction of a much smaller matrix of dimension $M \times M$.*

Acknowledgments

This work was supported in part by the joint research program MANON between CEA-Saclay and University Pierre et Marie Curie-Paris 6. It has also been supported by Fondation Sciences Mathematiques de Paris, that hosts Anthony Patera on the Foundation's Senior Research Chair.

[1] Y. Maday, O. Mula, A generalized empirical interpolation method: Application of reduced basis techniques to data assimilation, in: F. Brezzi, P. Colli Franzone, U. Gianazza, G. Gilardi (Eds.), Analysis and Numerics of Partial Differential Equations, Vol. 4 of Springer INdAM Series, Springer Milan, 2013, pp. 221–235.

[2] M. Barrault, Y. Maday, N. Nguyen, A. Patera, An empirical interpolation method: Application to efficient reduced-basis discretization of partial differential equations., C. R. Acad. Sci. Paris, Série I. 339 (2004) 667–672.

[3] M. Grepl, Y. Maday, N. Nguyen, A. Patera, Efficient reduced-basis treatment of nonaffine and nonlinear partial differential equations., ESAIM, Math. Model. Numer. Anal. 41(3) (2007) 575–605.

[4] Y. Maday, N. Nguyen, A. Patera, G. Pau, A general multipurpose interpolation procedure: the magic points, Comm. Pure Appl. Anal. 8(1) (2009) 383–404.

[5] A. Chkifa, A. Cohen, C. Schwab, High-dimensional adaptive sparse polynomial interpolation and applications to parametric PDE's, Foundations of Computational Mathematics (2013) 1–33.
[6] I. H. Sloan, Nonpolynomial interpolation, J. Approx. Theory 39 (2) (1983) 97 – 117.
[7] M. Floater, K. Hormann, Barycentric rational interpolation with no poles and high rates of approximation, Numer. Math. 107 (2) (2007) 315–331.
[8] J. Kleijnen, W. van Beers, Robustness of kriging when interpolating in random simulation with heterogeneous variances: Some experiments, European Journal of Operational Research 165 (3) (2005) 826 – 834.
[9] M. Drohman, B. Haasdonk, M. Ohlberger, Reduced Basis Approximation for Nonlinear Parametrized Evolution Equations based on Empirical Operator Interpolation, SIAM J. Sci. Comput. 34 (2012) A937–A969.
[10] A. Kolmogoroff, Über die beste Annäherung von Funktionen einer gegebenen Funktionenklasse, Annals of Mathematics 37 (1936) 107–110.
[11] Y. Maday, A. Patera, G. Turinici, A priori convergence theory for reduced-basis approximations of single-parameter elliptic partial differential equations, Journal of Scientific Computing 17 (1-4) (2002) 437–446.
[12] A. Cohen, R. DeVore, Kolmogorov widths under holomorphoc mappings, Submitted.
[13] Y. Maday, O. Mula, G. Turinici, A priori convergence of the Generalized Empirical Interpolation Method, in: 10th international conference on Sampling Theory and Applications (SampTA 2013), 2013, pp. 168–171.
[14] Y. Maday, O. Mula, G. Turinici, Convergence analysis of the Generalized Empirical Interpolation Method, Submitted – (2014) –.
[15] J. Eftang, A. Patera, E. Rønquist, An" hp" certified reduced basis method for parametrized elliptic partial differential equations, SIAM J. Sci. Comput. 32 (6) (2010) 3170–3200.
[16] J. Eftang, B. Stamm, Parameter multi-domain "hp" empirical interpolation, Int. J. Numer. Methods Eng. 90 (4) (2012) 412–428.
[17] Y. Maday, B. Stamm, Locally adaptive greedy approximations for anisotropic parameter reduced basis spaces., SIAM J. Sci. Comput. 35 (6).
[18] M. Yano, J. Penn, A. Patera, A model-data weak formulation for simultaneous estimation of state and model bias, Comptes Rendus Mathematique 351 (2324) (2013) 937 – 941.
[19] Y. Maday, A. Patera, J. Penn, M. Yano, A Parametrized-Background Data-Weak approach to variational data assimilation: formulation, analysis and application to accoustics, Int. J. Num. Meth. Eng.Submitted.
[20] A. Bennett, Array design by inverse methods, Vol. 15, 1985.
[21] A. Patera, E. Rønquist, Regression on parametric manifolds: Estimation of spatial fields, functional outputs, and parameters from noisy data, C.R. Acad. Sci. Paris Series I 350 (9-10) (2012) 543–547.